HHS Public Access

Author manuscript

Cancer Lett. Author manuscript; available in PMC 2022 May 28.

Published in final edited form as:

Cancer Lett. 2021 May 28; 506: 95–106. doi:10.1016/j.canlet.2021.03.002.

Interferon Regulatory Factor 1(IRF-1) activates anti-tumor immunity via CXCL10/CXCR3 axis in Hepatocellular Carcinoma (HCC)

Yihe Yan[1,2,*], **Leting Zheng**[2,3,*], **Qiang Du**[2], **Hamza Yazdani**[2], **Kun Dong**[2], **Yarong Guo**[2], **David A Geller**[2]

[1]Department of General Surgery, The Second Affiliated Hospital of Guangxi Medical University, Nanning, Guangxi 530007, China.

[2]Thomas E. Starzl Transplantation Institute, Department of Surgery, University of Pittsburgh Medical Center, Pittsburgh, PA 15260, USA.

[3]Department of Rheumatology and Immunology, The First Affiliated Hospital of Guangxi Medical University, Nanning, Guangxi 530021, China.

Abstract

Interferon regulatory factor 1 (IRF-1) is a tumor suppressor gene in cancer biology with anti-proliferative and pro-apoptotic effect on cancer cells, however mechanisms of IRF-1 regulating tumor microenvironment (TME) in hepatocellular carcinoma (HCC) remain only partially characterized. Here, we investigated that IRF-1 regulates C-X-C motif chemokine 10 (CXCL10) and chemokine receptor 3 (CXCR3) to activate anti-tumor immunity in HCC. We found that IRF-1 mRNA expression was positively correlated with CXCL10 and CXCR3 through qRT-PCR assay in HCC tumors and in analysis of the TCGA database. IRF-1 response elements were identified in the CXCL10 promoter region, and ChIP-qPCR confirmed IRF-1 binding to promote CXCL10 transcription. IRF-2 is a competitive antagonist for IRF-1 mediated transcriptional effects, and overexpression of IRF-2 decreased basal and IFN-γ induced CXCL10 expression. Although IRF-1 upregulated CXCR3 expression in HCC cells, it inhibited proliferation and exerted pro-apoptotic

Correspondence to: David A Geller; Thomas E. Starzl Transplantation Institute, Department of Surgery, University of Pittsburgh Medical Center, Pittsburgh, PA 15260, USA. Tel.: +1 412 692 2001; fax: +1 412 692 2002. gellerda@upmc.edu., Yihe Yan; Thomas E. Starzl Transplantation Institute, Department of Surgery, University of Pittsburgh Medical Center, Pittsburgh, PA 15260, USA. Tel.: +1 412 624 6702; fax: +1 412 624 6666. yiheyan@hotmail.com.

*Contributed equally

Author contributions

YY and DAG designed the research. YY, LZ, QD, HY, KD, and YG performed the experiments and also analyzed the data. YY and DAG wrote the manuscript. All authors edited and approved the submission of this work.

Disclosure of Potential Conflicts of Interest

No potential conflicts of interest were disclosed.

Ethics approval and consent to participate

Human tissue samples were obtained in accordance with the University of Pittsburgh Institutional Review Board (IRB) approved protocol (No. MOD08010372/PRO08010372). Animal experiments were approved by the University of Pittsburgh Institutional Animal Care and Use Committee (Protocol No. 18012053).

effects, which overcome proliferation partly mediated by activating the CXCL10/CXCR3 autocrine axis. In vitro and in vivo studies showed that IRF-1 increased CD8+ T cells, NK and NKT cells migration, and activated IFN-γ secretion in NK and NKT cells to induce tumor apoptosis through the CXCL10/CXCR3 paracrine axis. Conversely, this effect was markedly abrogated in HCC tumor bearing mice deficient in CXCR3. Therefore, the IRF-1/CXCL10/CXCR3 axis contributes to the anti-tumor microenvironment in HCC.

Keywords

Tumor microenvironment; IRF-1; Chemokine; Chemokine receptor; Hepatocellular carcinoma

1. Introduction

Hepatocellular carcinoma (HCC) ranks as the fifth most frequently diagnosed cancer worldwide [1]. Liver resection or liver transplantation remains the only curative options for patients with HCC. Unfortunately, most patients are diagnosed with advance disease and have poor prognosis [2]. For non-operative patients, regional liver therapies, systemic chemotherapy, and immune checkpoint blockade (ICB) are therapeutic options, although treatment resistance is high and clinical response rates are typically less than 50% [3, 4]. Advances in understanding signaling mechanisms in the HCC tumor microenvironment (TME) have led to progress with treatment options [5], yet many unknowns still exist for in the TME.

The Interferon pathway exerts multiple functions in the HCC TME with anti-proliferative and pro-apoptotic effects, as well as attenuating anti-tumor immunity through tumor cell-intrinsic and extrinsic factors [3]. Interferon regulatory factor 1 (IRF-1) is a master transcription factor in the Interferon-γ pathway [6]. IRF-1 exerts an anti-proliferative effect and promotes apoptosis, and also enhances immune cell recognition of tumors including colorectal, breast, and esophageal carcinoma, and HCC [7–13]. Our previous study identified IRF-1 as a tumor suppressor gene which promoted autophagy with growth inhibition and cell death of HCC cells [14]. Conversely, we also observed that IRF-1 upregulates PD-L1 expression to assist HCC cells in escaping from anti-tumor immunity [15]. Therefore, tumor derived IRF-1 regulates the TME to either activate or suppress anti-tumor immune response.

Chemokines are a family of small cytokines or signaling proteins secreted by various cells. They have been reported to promote an anti-tumor response in the TME and have shown clinical benefit in some cancer patients; however, some chemokines and chemokine receptors attenuate the therapeutic efficacy of immunotherapy and conventional therapy [5, 16]. CXCL9, −10, −11 are CXC chemokines, which are mainly secreted by monocytes, endothelial cells, fibroblasts, and cancer cells in response to IFN-γ, as well as being selective ligands for CXCR3. Their functions involve in regulating immune cell migration, differentiation, and activation for anti-tumor immunity by a paracrine axis [17, 18]. Conversely, CXCR3 is predominantly induced by IFN-γ and expressed on tumor cells. Tumor derived CXCL9,−10,−11 can increase its own proliferation, angiogenesis, and

metastasis due to autocrine signaling [17–20]. Therefore, the opposing effects of CXCL9,−10,−11 and CXCR3 in the tumor and TME may occur simultaneously.

CXCL10 has been shown to orchestrate anti-tumor immunity in certain cancers [21–24]. Higher CXCL10 and CXCR3 expression are positively correlated with a better clinical outcome of HCC patients in the Cancer Genome Atlas (TCGA) [25]. However, several studies show that CXCL10 in the TME decreases the anti-tumor immune response to promote HCC tumorigenesis and postoperative recurrence [26–28]. CXCL10 has also been shown to attract more immunosuppressive cells to the TME [28–30]. Accordingly, the effects of cross-talk between IRF-1 and CXCL10/CXCR3 pathway in regulating the HCC TME warrants further evaluation.

In this study, we show that IRF-1 upregulates CXCL10 expression in HCC cells at the transcriptional level. Endogenous IRF-1 promotes anti-proliferative and pro-apoptotic effect on HCC cells, which overcomes proliferation partly mediated by activating the CXCL10/CXCR3 autocrine pathway. Furthermore, tumor derived IRF-1 activates NK cells, NKT cells and CD8+ T cells enrichment, and enhances anti-tumor activity of NK cells and NKT cells through CXCL10/CXCR3 signaling. These novel findings show the importance of the IRF-1/CXCL10/CXCR3 axis in regulating the anti-tumor microenvironment in HCC.

2. Materials and Methods

2.1. Patient samples

Ten HCC tumor tissues were obtained from patients undergoing hepatectomy at the Liver Cancer Center of the University Of Pittsburgh School Of Medicine (Pittsburgh, PA, USA). These human tissues were acquired in accordance with a University of Pittsburgh Institutional Review Board (IRB) approved protocol (No. MOD08010372/PRO08010372).

2.2. Cell line and reagents

Liver cancer cell lines Hepa1–6, Huh-7 and HepG2 were obtained from ATCC (Manassas, VA, USA). Cells were cultured in Dulbecco's modified Eagle's medium (DMEM) (Lonza, Alpharetta, GA, USA), containing 10% heat-inactivated fetal bovine serum (FBS) (Clontech, Mountain View, CA, USA), 100 U/ml penicillin, 100 μg/ml streptomycin, 15 mmol/l HEPES and 200 mmol/l L-glutamine. The cells were maintained at 37°C in a humidified incubator containing 5% CO_2. Recombinant mouse and human IFN-γ were acquired from R&D (Minneapolis, MN, USA). Recombinant mouse IP 10 (CXCL10) was purchased from PROSPEC (Israeli). AMG 487 (CXCR3 inhibitor) was obtained from MCE (NJ, USA)

2.3. Mice and animal experiments

Female 5–6 weeks old wild type (WT) C57BL/6 (B6) mice (H-2b) and CXCR3 knock out (KO) mice (B6.129P2-CXCR3$^{tm1/Dgen}$/J) were purchased from the Jackson Laboratory (Bar Harbor, ME). Mice were raised in a specific pathogen-free environment under a temperature and light-controlled room with free access to food and water. Animal experiments were approved by the University of Pittsburgh Institutional Animal Care and Use Committee

(Protocol No. 18012053). Anesthesia was conducted with isoflurane (Piramal Critical Care, PA, USA). B6 mice were injected with 1×10^7 Hepa1–6 cells subcutaneously in the left flank containing 100 μl growth factor depleted Matrigel (CORNING, MA, USA). Tumor size was calculated every 3 days by caliper. Tumor volume=L×W× ((L+W)/2). Body weight was recorded every 3 days. After 2 weeks, mice were sacrificed under anesthesia by cervical dislocation. Tumors were harvested for single cell suspension for flow cytometry or frozen with OCT, and 5 μM sections were cut.

2.4. Adenovirus infection

An E1- and E3- deficient adenoviral vector carrying the mouse or human AdIRF-1, AdIRF-2, AdLacz, or Adψ5 cDNA was constructed as previously depicted [11, 15]. Hepa1–6 and Huh-7 cells were transduced with adenoviral concentration of 50 MOI for 48 h. 48 h after infection, cells were collected, and then total RNA and cell lysate protein and nuclear protein were extracted, respectively.

2.5. Transfection

The murine IRF-1 siRNA (sc-35707) and human IRF-1 siRNA (sc-35706) and control siRNA (sc-37007) were acquired from Santa Cruz Biotech. The cells were seeded in a 6 well plate and the following day transfected with Lipofectamine RNAiMAX (Invitrogen, Carlsbad, CA, USA). Serum-free medium was replaced with growth medium after 8 h. 36 h after transfection, IFN-γ was added or not. 48 h after transfection, culture medium and cells were respectively collected to analyze the protein level using ELISA assay.

2.6. Real-time RT-PCR

Total RNA was isolated with TRIzol reagent (Invitrogen, Carlsbad, CA, USA) and reversely transcribed to single-stranded cDNA with RNA to cDNA EcoDry™ Premix Kit (Takara, Kusatsu, Shiga Prefecture, Japan). Real-time polymerase chain reaction (PCR) was conducted using SYBR Premix Kit (Takara) on the ABI Stepone PCRSystem (Applied Biosystems, Foster City, CA, USA). Relative expression of each gene was normalized to β-actin mRNA or GAPDH mRNA for mouse and human samples, respectively. Primer sequences used are described in Supplemental Table 1.

2.7. Western blot

Total cell lysates and nuclear proteins were isolated according to previous study [31]. A total of 30ug nuclear protein or 60ug cell lysate was electrophoresed on 10% SDS-polyacrylamide gels and transferred to polyvinylidene difluoride membranes. The membranes were incubated with a 1:1000 dilution of primary antibodies overnight. Antibodies used for western blot contained anti-IRF1 (#8478), PARP (#9352) and LaminA/C antibodies (#4777) (CST, MA, USA); anti-CXCR3 (ab181013) and β-actin (ab8227) antibodies (abcam, MA, USA). IRDye 800CW anti-mouse and 680RD anti-rabbit secondary antibodies were obtained from LI-COR (Lincoln, USA). After wash with Tris-buffered saline and Tween-20 (TBST) for three times, membranes were incubated with a 1:5,000 dilution of secondary antibody for 30 min and scanned by Li-Cor odyssey. The β-

actin or LaminA/C protein was respectively used as standardization of cell lysate or nuclear protein.

2.8. Immunofluorescent staining and flow cytometry

Immunofluorescent staining was conducted as previously described [32]. Tissues were fixed with 2% paraformaldehyde in phosphate-buffered saline (PBS) for 2 h, and then dehydrated by 30% sucrose in PBS overnight. Cells were cultured on coverslips, fixed with 4% paraformaldehyde in PBS for 15 min. The tissues or cells were permeabilized with 0.1% Triton X-100 and 10% FBS in PBS for 30 min at room temperature, and incubated with primary antibody. Anti-CXCL10 (ab8098, abcam), CXCR3 (ab181013), CD8a (Clone: 53–6.7, Biolegend), and NK1.1 antibodies (Clone: PK136, Biolegend) were used. Alexa Fluor 594 anti-rabbit or 488 anti-mouse secondary antibodies were applied. After washing with PBS, slides were stained with 4',6-diamidine-2'-phenylindole dihydrochloride (DAPI) and mounted, and then observed using a Olympus Fluoview FV1000 III microscope (Olympus, Tokyo, Japan).

Single cell suspension was acquired from collected tumor tissues. The staining was conducted according to standard protocol for flow cytometry with anti-mouse CD3 (Clone: 17A2, Biolegend), CD4 (Clone: GK1.5, BD Horizon™), CD8a (Clone: 53–6.7, BD Horizon™), NK1.1 (Clone: PK136, Biolegend), CD19 (Clone: 1D3 RUO, BD Horizon™), CXCR3 (Clone: CXCR3–173, Biolegend) and IFN-γ (Clone: XMG1.2 RUO, BD Horizon™) antibodies. For detection of IFN-γ, single cells were cultured for 3 h with PMA (100 ng/ml), ionomycin (1000 ng/ml; both from Sigma-Aldrich), and GolgiPlug (1 μl/ml; BD Biosciences). Intracellular IFN-γ staining was performed after permeabilization using intracellular staining kits from BD Biosciences and eBioscience. Flow cytometry was carried out to analyze cellular apoptosis by APC Annexin V Apoptosis Detection Kit with PI (640932, BioLegend). The data were acquired on BD™ LSR II and analyzed with FlowJo software (version 10.6.1).

2.9. Chromatin Immunoprecipitation (ChIP)

ChIP-IT® Express Enzymatic Magnetic Chromatin Immunoprecipitation Kit & Enzymatic Shearing Kit (Active Motif) was used for the ChIP assay. We designed 7 pairs of qPCR primers in the human CXCL10 transcript promoter region (Supplemental Table 1). Huh-7 cells were collected after 250 U/ml IFN-γ 6 hours treatment. The ChIP procedure was performed according to the manufacturer's protocol. Chromatins were sheared 5 minutes with enzyme provided by kit. Anti IRF-1 antibody (ab26109, abcam, ChIP grade) was used in the experiment. The qPCR was performed to detect DNA collected by ChIP.

2.10. ELISA

Murine and human CXCL10 were quantified using enzyme-linked immunosorbent assay (ELISA) kits (Invitrogen, MD, USA) according to the manufacturer's protocol.

2.11. Establishment of IRF-1 stably expressing cells

Mouse IRF-1 ORF clone (NM001159396, #MR204833) and empty vector pCMV6-Entry (#PS100001) were purchased from OriGene (Rockville, MD, USA). Hepa1–6 cells were

seeded and the following day transfected with Lipofectamine 2000 (Invitrogen, Carlsbad, CA, USA). 48 h after transfection, transfected cells were selected by 1400 μg/ml G418 (#11811031, Gibco, USA). Next, single clone with G418 resistance was picked and expanded. Clones were subsequently screen by qRT-PCR and Western blotting for IRF-1 mRNA and protein expression.

2.12. Cell growth assay (MTT)

For cell growth assay, cells were seeded in 200 μl medium per well at 1×10^3 in 96-well plates. 3-(4, 5-Dimethylthiazol-2-yl)-2, 5- diphenyltetrazolium bromide (MTT) assay was carried out to evaluate cell growth according to the manual (ab211091, abcam). The absorbance was determined at 590 nm.

2.13. Transwell migration assay

Splenocytes were isolated from HCC tumor mice as previous study [15]. Splenocytes were resuspended in RPMI 1640 medium without serum and seeded in the upper chamber of a 8-μm pore size transwell 24 well plate (Corning Incorporated, Corning, ME, USA), 1×10^6 cells/well. Hepa1–6 cells with IRF-1 stably expressing or negative control were seeded in the lower chambers filled with DMEM medium added with 10% serum, 1×10^5 cells/well. After 24 h, the number of cells that migrated to the lower chamber was counted by flow cytometry.

2.14. Luciferase assays

Firefly luciferase reporter pGL4 plasmids expressing the wild-type or mutated interferon stimulated responsive element (ISRE) CXCL10 promoter were provided by David Proud [33–35]. The β-gal reporter control plasmid was used to normalize the transfection efficiency. HepG2 were cultured in 12-well plates and co-transfected with β-gal and either pGL4 empty vector or CXCL10 promoter luciferase reporter constructs using lipofectamine 2000 (Invitrogen). Serum-free medium was replaced with growth medium after 6h. 24 h after transfection, cells were induced by IFN-γ or infected with either Adψ5, AdIRF-2, or combo for 24 h. 48 h after transfection, the cells were lysed. Relative luciferase and β-galactosidase activities were measured with the reporter lysis buffer and luciferase substrate (Promega). The relative luciferase unit (RLU) was measured using the Dual-Luciferase Report Assay (BioTek, Winooski, VT, USA).

2.15. Statistical analysis

Statistical analyses were performed using GraphPad Prism 8 software (GraphPad Software Inc, San Diego, CA). To test for statistical significance, Student’s t test was used to compare between two different groups. One-way ANOVA analysis was performed to compare more than two different groups. Results are collective data from 2 to 4 independent experiments. Data are described by mean values ± standard deviation (SD), unless otherwise specified. For all analyses, $p < 0.05$ was considered significant.

3. Results

3.1. IRF-1 upregulates CXCL10 expression in HCC cells.

To investigate the correlation of IRF-1 and CXCL10 in human HCC, we checked IRF-1 and CXCL10 mRNA expression in resected HCC tumors. Our data showed that IRF-1 mRNA expression positively correlated with CXCL10 (Fig. 1A). To confirm the correlation with a larger sample size, we analyzed the interaction of IRF-1 and CXCL10 mRNA expression in HCC tumors from The Cancer Genome Atlas (TCGA) data through cBioPortal [36, 37]. As predicted, IRF-1 mRNA expression was positively related with CXCL10 (Fig. 1B).

To investigate whether IRF-1 was an upstream regulator of CXCL10, we stimulated HCC cell lines with IFN-γ. We found that both IRF-1 and CXCL10 mRNA expression were increased in mouse Hepa1–6 (Fig. 1C) and human Huh-7 (Fig. 1E) HCC cell lines induced by IFN-γ. Furthermore, exogenous IRF-1 specifically upregulated CXCL10 mRNA expression in HCC cells through adenoviral IRF-1 (AdIRF-1) transduction (Fig. 1D, 1F).

To explore whether IRF-1 had an effect on CXCL10 protein expression, we analyzed CXCL10 level by ELISA. We found that CXCL10 protein level was markedly increased in both cell culture medium and lysis of HCC cell lines infected by AdIRF-1, but not Adψ5 control (Fig. 1G, 1H). Conversely, silencing of endogenous IRF-1 expression using IRF-1 siRNA in Hepa1–6 and Huh-7 cells decreased basal CXCL10 level, as well as attenuated increased CXCL10 expression induced by IFN-γ (Fig.1I, 1J). Accordingly, these findings are consistent with the notion that IRF-1 induces CXCL10 expression in HCC cells.

3.2. IRF-2 blocks CXCL10 transcription.

Since IRF-1 is a master transcription factor in the IFN-γ pathway, we investigated whether IRF-1 upregulates CXCL10 at the transcriptional level. IRF-2 competes with IRF-1 for binding to the same regulatory elements of IFN inducible genes to block IRF-1 mediated transcriptional effects [15, 38]. Therefore, we first transduced HCC cell lines with AdIRF-2 and found a decreased CXCL10 basal and IFN-γ induced mRNA expression in mouse Hepa1–6 (Fig. 2A) and human Huh-7 (Fig. 2B)

3.3. IRF-1 response element in the CXCL10 promoter

To define the molecular mechanisms of IRF-1 regulating CXCL10 transcription, we analyzed two kilobases in the 5'-upstream flanking region of the human CXCL10 gene using PROMO bioinformatics software. We identified seven putative IRF-1 binding elements (B1-B7) in the human CXCL10 promoter. Noteworthy is that two elements at −179 and −51 nucleotides were conserved in human and murine sequences (Fig. 2C). Since a previous study also showed that epithelial production of CXCL10 was dependent upon IRF-1 [34], we first confirmed that luciferase activity of wild-type CXCL10 promoter plasmid (but not mutated ISRE) was enhanced in HCC cells induced by IFN-γ (Fig. 2E). Sequences of ISRE motif and mutated ISRE (mISRE) motif in human CXCL10 promoter are indicated (Supplementary Fig. 1A). We then found that IRF-2 expression significantly decreased IFN-γ stimulated CXCL10 promoter activity (Fig. 2F).

To discover whether IRF-1 directly binds to CXCL10 promoter and specifically which binding elements were functionally active, we conducted chromatin immunoprecipitation (ChIP) in the cell lysis of Huh-7 cells with anti-IRF1 antibody and PCR primers spanning each element. IFN-γ induced IRF-1 transcriptional activity was observed with anti-IRF1 Ab (but not control IgG Ab) for binding at B4 and B7 response elements (Fig. 2D). However, no transcriptional binding was seen at the other putative ISRE elements. These data are consistent with the notion that IFN-γ induces CXCL10 transcription by inducing IRF-1 which binds to IRF-1 response elements at −853 and −51 nucleotides in the CXCL10 promoter region. Taken together, these results showed that IRF-1 promotes CXCL10 transcription in HCC cells.

3.4. IRF-1 exerts anti-proliferative and pro-apoptotic effect on HCC cells.

Since CXCR3 is induced by IFN-γ and is expressed on tumor cells, we investigated the interaction of IRF-1 and CXCR3 in HCC. We first found IRF-1 mRNA expression positively correlated with CXCR3 in our HCC samples (Fig. 3A) and same result was observed from the TCGA database (Fig. 3B). In addition, exogenous IRF-1 enhanced CXCR3 mRNA and protein expression in HCC cells (Fig. 3C, 3D). The full uncut gels are shown in Supplemental Figure 4.

Since CXCR3 is induced by IRF-1, and CXCL10 increases tumor proliferation by binding to CXCR3 via autocrine signaling [17–19], we first confirmed that CXCL10 (IP10) enhances HCC cells proliferation using MTT assay in murine HCC Hepa1–6 cells induced by murine CXCL10 (Supplementary Fig. 1B). Conversely, CXCR3 inhibitor (AMG 487) abrogated the increased proliferation induced by CXCL10. We then determined whether exogenous IRF-1 has pro-tumorigenic or anti-tumor effects on HCC cells. We constructed a Hepa1–6 murine HCC cell line which was stably transfected with an expression construct encoding IRF-1. We confirmed strong IRF-1 nuclear protein expression in the stably transformed cells (but not negative control empty vector) (Supplementary Fig. 1C). Likewise, strong IRF-1 mRNA and total protein expression was observed in the HCC cells stably transformed to express IRF-1 (Fig. 3E). CXCL10 and CXCR3 mRNA expression were increased in the IRF-1 overexpressing cells (Fig. 3F). Furthermore, immunofluorescent staining for CXCL10 (green) and CXCR3 (red) proteins confirmed that both were upregulated (Fig. 3G).

We next delineated proliferative and apoptotic characteristics of HCC cells with exogenous over-expression of IRF-1. Flow cytometry showed increased apoptosis in HCC cells overexpressing IRF-1 (Fig. 3H, 3I). Moreover, decreased cellular proliferation was observed in Hepa1–6 cells overexpressing IRF-1 (Fig. 3J). To confirm that the pro-apoptotic effect of IRF-1 was not specific to murine HCC, we also examined the effect of IRF-1 expression on apoptosis in the human HCC cell line Huh-7. AdIRF-1 (but not AdLacZ) transduction increased cleaved PARP, a marker of apoptosis (Fig. 3K). Accordingly, HCC cells with overexpressed IRF-1 demonstrated increased apoptosis and decreased proliferation, which overcome proliferation partly mediated by the IFN-γ/IRF-1/CXCL10/CXCR3 autocrine axis.

3.5. Tumor derived IRF-1 recruits and activates immune cells to enhance apoptosis in murine HCC tumor

IRF-1 induces a number of immunomodulatory mediators including MHC-I, MHC-II, IL-15, and inducible NO synthase (iNOS) suggesting that IRF-1 is involved in upregulation of antigen presentation to prime anti-tumor immunity [7, 10, 39]. On the other hand, our previous studies demonstrated that IRF-1 expression was considered a double-edged sword in HCC tumors with increased PD-L1 expression resulting in attenuation of antitumor immunity under certain inflammatory conditions [15]. Therefore, we investigated the role of IRF-1 in regulating the TME in HCC.

Transwell migration assays using mouse splenocytes and HCC cells showed an increased number of CD3+, CD4+, CD8+ T lymphocytes (Fig. 4A), and NK and NKT cells (Fig. 4B) in the culture medium of HCC cells expressing IRF-1 determined by flow cytometry (Supplementary Fig.2).

We then injected IRF-1 overexpressing Hepa1–6 cells subcutaneously into B6 mice. Growth inhibition was observed in tumors with overexpressed IRF-1 (Fig. 4C). Flow cytometry showed increased apoptosis in vivo in the subcutaneous HCC tumors overexpressing IRF-1 (Fig. 4D, 4E). Furthermore, significantly more infiltrating NK cells and NKT cells, as well as CD3+ and CD8+ T cells were recruited into the tumor by IRF-1 overexpression (Fig. 4G–4K), whereas no apparent change in infiltrating CD19+ B cells were found (Fig. 4G, 4I). Meanwhile, significantly increased CD8a mRNA expression was observed in the tumors with upregulated IRF-1 (Fig. 4F).

We next defined the activity of these recruited immune cells. Increased granzyme B (GZMB) and IFN-γ mRNA expression were observed in IRF-1 expressing tumors (Fig. 4F). In addition, flow cytometry showed significantly increased IFN-γ expression in infiltrating NK and NKT cells of HCC tumor with upregulated IRF-1 (Fig. 5A, 5B, 5F); however, no statistical difference was found in IFN-γ expression from infiltrating CD3+, CD4+, or CD8+T cells in the tumor (Fig. 5C–5E, 5G). Therefore, we conclude that murine HCC cells with stable expression of IRF-1 recruit NK cells, NKT cells, and CD8+ T cells into the tumor, as well as activate NK and NKT cells to secrete IFN-γ to induce HCC cellular apoptosis.

3.6. IRF-1 activates anti-tumor immunity via CXCL10/CXCR3 axis in the murine HCC tumor

Since CXCR3 is expressed on immune cells including T lymphocytes and NK cells, and CXCL10 binds to CXCR3 [17, 18, 40, 41], we next determined whether IRF-1 recruits and activates T lymphocytes and NK cells through the CXCL10/CXCR3 paracrine axis. We first confirmed that CXCL10 and CXCR3 mRNA expression is increased in murine HCC tumor overexpressing IRF-1 (Fig. 6A). We then investigated whether CXCR3+ T lymphocytes, NK and NKT cells were infiltrating into these IRF-1 overexpressing tumors. Flow cytometry showed significantly increased infiltrating CXCR3+ CD8+ T cells, NK cells and NKT cells in tumors overexpressing IRF-1 (Fig. 6B–6F). Furthermore, immunofluorescent staining for

CXCR3, CD8A and NK1.1 supports increased infiltrating CXCR3+ CD8+T cells and NK cells in IRF-1 overexpressing tumors (Supplementary Fig.3A, 3B).

To determine if CXCR3 in immune cells binds to CXCL10 secreted by IRF-1 expressing tumor cells, we injected HCC cells into CXCR3 wild type (WT) and knock out (KO) mice. Consistent with our earlier findings, tumors were smaller in WT mice that had tumor overexpression of IRF-1 (Fig. 7A, rows 1 and 3). Of note, CXCR3 KO mice showed larger tumors compared to WT mice (Fig. 7A, rows 1 and 2), consistent with the notion that CXCR3 mediated immune cell recruitment and activation combats tumors. The CXCR3 KO mice bearing tumors with overexpression of IRF-1 showed increased tumor size compared to WT mice overexpressing IRF-1 (Fig. 7A, rows 3 and 4), indicating a partial dependence of IRF-1 on recruited immune cells to mediate anti-tumor effects. In order to investigate changes of infiltrating immune cells in WT and CXCR3 KO mice, we counted the number of tumor-infiltrating immune cells in the whole tumor. IRF-1 overexpressing tumors showed increased infiltrating NK and NKT cells, and this was abrogated in CXCR3 KO mice compared to WT mice (Fig. 7B, 7C). Meanwhile, the infiltrating CD3+ and CD8+ T cells were significantly decreased in CXCR3 KO mice vs. WT mice (Fig. 7D, 7E). Similar to earlier findings (Fig. 4H), CD4+ T cells in tumors with overexpression of IRF-1 showed a modest increase in tumor from CXCR3 KO mice and WT mice (Fig. 7F).

Since IFN-γ expression in NK and NKT cells was significantly increased in tumors overexpressing IRF-1 (Fig. 5F), to define whether anti-tumor function of NK and NKT cells was altered in tumors with IRF-1 overexpressed in CXCR3 KO mice, we conducted IFN-γ staining in NK cells and NKT cells. We found increased infiltrating IFN-γ+ NK cells and NKT cells in tumors overexpressing IRF-1 which was attenuated in CXCR3 KO mice vs. WT mice (Fig. 7G, 7H).

A summary diagram (Fig. 8) in HCC tumor cells illustrates that IRF-1 promotes CXCL10 expression at the transcriptional level. The induced CXCL10 binds to CXCR3 in the tumor cells via an autocrine axis. Meanwhile, immune cells including NK cells, NKT cells, and CD8+T cells are recruited, and NK cells and NKT cells are activated to produce IFN-γ resulting in a paracrine IFN-γ/IRF-1/CXCL10/CXCR3 axis that promotes apoptosis and inhibits tumor cell proliferation in HCC.

4. Discussion

The major finding of this study is that the IRF-1/CXCL10/CXCR3 axis contributes to the anti-tumor microenvironment in HCC. IRF-1 mRNA expression positively correlated with CXCL10 and CXCR3 in HCC tumors. The mechanism involved IRF-1 binding to IRF-1 response elements identified in the CXCL10 promoter region, and ChIP assay confirmed IRF-1 binding to promote CXCL10 transcription. IRF-2 is a competitive antagonist for IRF-1 mediated transcriptional effects, and IRF-2 expression decreased basal and IFN-γ induced CXCL10 expression. Although IRF-1 upregulated CXCR3 expression in HCC cells, it inhibited proliferation and exerted pro-apoptotic effects, which countered the proliferative effects partly mediated by activating the CXCL10/CXCR3 autocrine axis. In vitro and in vivo studies showed that IRF-1 increased CD8+ T cells, NK and NKT cells migration, and

activated IFN-γ secretion in NK and NKT cells to induce tumor apoptosis through the CXCL10/CXCR3 paracrine axis. These effects were markedly abrogated in HCC tumor bearing mice deficient in CXCR3. Hence, these findings define an important role for IRF-1/CXCL10/CXCR3 signaling in the HCC TME. Currently, combining molecular targeted approaches with ICB to treat HCC patients in has been promising [42]. However, many HCC patients are resistant to these combined therapies. Mechanism of resistance involve cross-talk between tumor cells and the TME [3, 43]. TME in malignant tumors exhibiting resistance to therapy usually demonstrate suppressive anti-tumor immune cells, chemokines and cytokines [5, 43]. Our study sought to define the role of CXCL10/CXCR3 signaling in HCC cells, and the mechanisms governing the tumor response in the TME.

IRF-1 functions as a tumor suppressor gene inhibiting proliferation and promoting apoptosis of tumor cells. The mechanisms of IRF-1 triggering growth arrest and apoptosis rely on its ability as a transcription factor to induce a number of genes that exert growth inhibitory and pro-apoptotic effects. Among them are p21 (WAF1), indoleamine 2,3-dioxigenase, caspase-1, -3, -7, -8, iNOS, IFN-α, and TNF-related apoptosis-inducing ligand (TRAIL), as well as IFN-γ-mediated enhancement of Fas/CD95-induced apoptosis [7–9, 11–13]. However, IRF-1 induced PD-L1 expression which attenuates anti-tumor immunity has been observed in cancers including HCC [15, 44, 45]. Therefore, IRF-1 exerts dueling roles in cross-talk regulating tumor immunology. Here, our study showed that HCC tumor derived IRF-1 activates immune cells to induce apoptosis of tumor cells through the CXCL10/CXCR3 axis in murine HCC tumor. The specific mechanism involves IRF-1 promoting CXCL10 transcription to recruit CXCR3+ CD8+ T cells, NK cells and NKT cells which activates anti-tumor effects of NK cells and NKT cells through increased IFN-γ expression.

One caveat is that our in vivo study was based on murine HCC tumor. Although human IRF-1 mRNA expression significantly positively correlated with CXCL10 and CXCR3, as well as with CD8a, GZMB, and IFN-γ gene expression in HCC samples according to our data or the TCGA database, additional studies using a human HCC tumor model are warranted to further define the role of the CXCL10/CXCR3 axis in regulating the anti-tumor immune response.

Tumor derived CXCL10 in response to chemotherapy plays an important role for anti-tumor T cells responses [24]; however, CXCL10 may also suppress anti-tumor immunity through priming of regulatory T cells, regulatory B cells, or plasma cells via binding to CXCR3 [27, 28, 30]. In our study, no significant difference was observed in B cells infiltrating into tumors overexpressing IRF-1. Another limitation of our study is that we did not examine for infiltrating regulatory T cells or plasma cells. However, the results show the importance of the IRF-1/CXCL10/CXCR3 paracrine axis and anti-tumor response of immune cells in subcutaneously grown murine HCC tumors expressing IRF-1. Consistent with this effect, higher CXCL10 and CXCR3 expression predicted a better prognosis of HCC patients according to the TCGA database [25].

In addition, we found that active IRF-1/CXCL10/CXCR3 expression promoted an inflammatory TME, manifested as increased infiltrating immune cells and active anti-tumor function with increased IFN-γ and GZMB levels, which are potentially beneficial for ICB

therapy [46, 47]. Some recent studies show that intra-tumoral CXCR3 chemokine serves as a biomarker for sensitivity to ICB therapeutics since that promotion of CXCR3-mediated signaling pathway may improve effectiveness of ICB treatment in tumors [48, 49]. However, whether coordinated expression of IRF-1, CXCL10 and CXCR3 can be considered a valuable biomarker to predict immunotherapy response in human HCC will require additional studies.

An additional finding of this study is that IRF-1 expression positively correlated with CXCR3, and CXCR3 is induced by IRF-1 in HCC. The mechanism of IRF-1 enhancing CXCR3 mRNA and protein expression likely relies in part on its pleiotropic transcriptional effects. We analyzed two kilobases in the 5'-upstream flanking region of the human CXCR3 gene using PROMO bioinformatics software and identified IRF-1 response elements (IRE) in the CXCR3 promoter region. However, the direct evidence that IRF-1 promotes CXCR3 by binding to a specific IRE will require future studies. The increased CXCR3 in tumor cells can considered pro-tumorigenic due to autocrine effects promoting cellular proliferation, metastasis, and angiogenesis [17–20]. In contrast, our findings confirmed that IRF-1 upregulation in HCC exerted pro-apoptotic and anti-proliferative effect on tumor cells, which overcame any proliferative effects. Increased CXCR3 expression in HCC cells has been shown to confer molecular targeted therapeutic resistance in HCC [50]. Whether CXCR3 expression could be induced by ICB therapy resulting in resistance requires further study.

Supplementary Material

Refer to Web version on PubMed Central for supplementary material.

Funding

This work was supported by the NIH Grant (HHSN276201200017C and P30DK120531-01, DAG), and the Guangxi Natural Science Foundation (2017GXNSFAA198014 and 2020GXNSFAA297008, Y.Yan).

Abbreviations

IRF-1	interferon regulatory factor 1
IRF-2	interferon regulatory factor 2
IFN-γ	interferon- γ
CXCL10	C-X-C motif chemokine 10
CXCR3	chemokine receptor 3
HCC	hepatocellular carcinoma
TME	tumor microenvironment
ICB	immune checkpoint blockade
PD-L1	programmed death-ligand 1

TCGA	the Cancer Genome Atlas
ELISA	enzyme-linked immunosorbent assay
NK cell	natural killer cell
NKT cell	natural killer T cell
MHC	major histocompatibility complex
IL	interleukin

Reference

[1]. Torre LA, Bray F, Siegel RL, Ferlay J, Lortet-Tieulent J, Jemal A, Global cancer statistics, 2012, CA Cancer J Clin, 65 (2015) 87–108. [PubMed: 25651787]

[2]. Liu Z, Lin Y, Zhang J, Zhang Y, Li Y, Liu Z, Li Q, Luo M, Liang R, Ye J, Molecular targeted and immune checkpoint therapy for advanced hepatocellular carcinoma, J Exp Clin Cancer Res, 38 (2019) 447. [PubMed: 31684985]

[3]. Sharma P, Hu-Lieskovan S, Wargo JA, Ribas A, Primary, Adaptive, and Acquired Resistance to Cancer Immunotherapy, Cell, 168 (2017) 707–723. [PubMed: 28187290]

[4]. Chen S, Cao Q, Wen W, Wang H, Targeted therapy for hepatocellular carcinoma: Challenges and opportunities, Cancer Lett, 460 (2019) 1–9. [PubMed: 31207320]

[5]. Galon J, Bruni D, Tumor Immunology and Tumor Evolution: Intertwined Histories, Immunity, 52 (2020) 55–81. [PubMed: 31940273]

[6]. Tamura T, Yanai H, Savitsky D, Taniguchi T, The IRF family transcription factors in immunity and oncogenesis, Annu Rev Immunol, 26 (2008) 535–584. [PubMed: 18303999]

[7]. Kroger A, Ortmann D, Krohne TU, Mohr L, Blum HE, Hauser H, Geissler M, Growth suppression of the hepatocellular carcinoma cell line Hepa1–6 by an activatable interferon regulatory factor-1 in mice, Cancer Res, 61 (2001) 2609–2617. [PubMed: 11289138]

[8]. Ohsugi T, Yamaguchi K, Zhu C, Ikenoue T, Takane K, Shinozaki M, Tsurita G, Yano H, Furukawa Y, Anti-apoptotic effect by the suppression of IRF1 as a downstream of Wnt/beta-catenin signaling in colorectal cancer cells, Oncogene, 38 (2019) 6051–6064. [PubMed: 31292489]

[9]. Stang MT, Armstrong MJ, Watson GA, Sung KY, Liu Y, Ren B, Yim JH, Interferon regulatory factor-1-induced apoptosis mediated by a ligand-independent fas-associated death domain pathway in breast cancer cells, Oncogene, 26 (2007) 6420–6430. [PubMed: 17452973]

[10]. Yang MQ, Du Q, Varley PR, Goswami J, Liang Z, Wang R, Li H, Stolz DB, Geller DA, Interferon regulatory factor 1 priming of tumour-derived exosomes enhances the antitumour immune response, Br J Cancer, 118 (2018) 62–71. [PubMed: 29112686]

[11]. Kim PK, Armstrong M, Liu Y, Yan P, Bucher B, Zuckerbraun BS, Gambotto A, Billiar TR, Yim JH, IRF-1 expression induces apoptosis and inhibits tumor growth in mouse mammary cancer cells in vitro and in vivo, Oncogene, 23 (2004) 1125–1135. [PubMed: 14762441]

[12]. Huang J, Li J, Li Y, Lu Z, Che Y, Mao S, Lei Y, Zang R, Zheng S, Liu C, Wang X, Li N, Sun N, He J, Interferon-inducible lncRNA IRF1-AS represses esophageal squamous cell carcinoma by promoting interferon response, Cancer Lett, 459 (2019) 86–99. [PubMed: 31173852]

[13]. Jeong SI, Kim JW, Ko KP, Ryu BK, Lee MG, Kim HJ, Chi SG, XAF1 forms a positive feedback loop with IRF-1 to drive apoptotic stress response and suppress tumorigenesis, Cell Death Dis, 9 (2018) 806. [PubMed: 30042418]

[14]. Li P, Du Q, Cao Z, Guo Z, Evankovich J, Yan W, Chang Y, Shao L, Stolz DB, Tsung A, Geller DA, Interferon-gamma induces autophagy with growth inhibition and cell death in human hepatocellular carcinoma (HCC) cells through interferon-regulatory factor-1 (IRF-1), Cancer Lett, 314 (2012) 213–222. [PubMed: 22056812]

[15]. Yan Y, Zheng L, Du Q, Yan B, Geller DA, Interferon regulatory factor 1 (IRF-1) and IRF-2 regulate PD-L1 expression in hepatocellular carcinoma (HCC) cells, Cancer Immunol Immunother, (2020).

[16]. Nagarsheth N, Wicha MS, Zou W, Chemokines in the cancer microenvironment and their relevance in cancer immunotherapy, Nat Rev Immunol, 17 (2017) 559–572. [PubMed: 28555670]

[17]. Tokunaga R, Zhang W, Naseem M, Puccini A, Berger MD, Soni S, McSkane M, Baba H, Lenz HJ, CXCL9, CXCL10, CXCL11/CXCR3 axis for immune activation - A target for novel cancer therapy, Cancer Treat Rev, 63 (2018) 40–47. [PubMed: 29207310]

[18]. Reynders N, Abboud D, Baragli A, Noman MZ, Rogister B, Niclou SP, Heveker N, Janji B, Hanson J, Szpakowska M, Chevigne A, The Distinct Roles of CXCR3 Variants and Their Ligands in the Tumor Microenvironment, Cells, 8 (2019).

[19]. Cambien B, Karimdjee BF, Richard-Fiardo P, Bziouech H, Barthel R, Millet MA, Martini V, Birnbaum D, Scoazec JY, Abello J, Al Saati T, Johnson MG, Sullivan TJ, Medina JC, Collins TL, Schmid-Alliana A, Schmid-Antomarchi H, Organ-specific inhibition of metastatic colon carcinoma by CXCR3 antagonism, Br J Cancer, 100 (2009) 1755–1764. [PubMed: 19436305]

[20]. Walser TC, Rifat S, Ma X, Kundu N, Ward C, Goloubeva O, Johnson MG, Medina JC, Collins TL, Fulton AM, Antagonism of CXCR3 inhibits lung metastasis in a murine model of metastatic breast cancer, Cancer Res, 66 (2006) 7701–7707. [PubMed: 16885372]

[21]. Brownell J, Polyak SJ, Molecular pathways: hepatitis C virus, CXCL10, and the inflammatory road to liver cancer, Clin Cancer Res, 19 (2013) 1347–1352. [PubMed: 23322900]

[22]. Wennerberg E, Kremer V, Childs R, Lundqvist A, CXCL10-induced migration of adoptively transferred human natural killer cells toward solid tumors causes regression of tumor growth in vivo, Cancer Immunol Immunother, 64 (2015) 225–235. [PubMed: 25344904]

[23]. Bronger H, Singer J, Windmuller C, Reuning U, Zech D, Delbridge C, Dorn J, Kiechle M, Schmalfeldt B, Schmitt M, Avril S, CXCL9 and CXCL10 predict survival and are regulated by cyclooxygenase inhibition in advanced serous ovarian cancer, Br J Cancer, 115 (2016) 553–563. [PubMed: 27490802]

[24]. Sistigu A, Yamazaki T, Vacchelli E, Chaba K, Enot DP, Adam J, Vitale I, Goubar A, Baracco EE, Remedios C, Fend L, Hannani D, Aymeric L, Ma Y, Niso-Santano M, Kepp O, Schultze JL, Tuting T, Belardelli F, Bracci L, La Sorsa V, Ziccheddu G, Sestili P, Urbani F, Delorenzi M, Lacroix-Triki M, Quidville V, Conforti R, Spano JP, Pusztai L, Poirier-Colame V, Delaloge S, Penault-Llorca F, Ladoire S, Arnould L, Cyrta J, Dessoliers MC, Eggermont A, Bianchi ME, Pittet M, Engblom C, Pfirschke C, Preville X, Uze G, Schreiber RD, Chow MT, Smyth MJ, Proietti E, Andre F, Kroemer G, Zitvogel L, Cancer cell-autonomous contribution of type I interferon signaling to the efficacy of chemotherapy, Nat Med, 20 (2014) 1301–1309. [PubMed: 25344738]

[25]. Zhang J, Chen J, Guan GW, Zhang T, Lu FM, Chen XM, [Expression and clinical significance of chemokine CXCL10 and its receptor CXCR3 in hepatocellular carcinoma], Beijing Da Xue Xue Bao Yi Xue Ban, 51 (2019) 402–408. [PubMed: 31209409]

[26]. He Y, Hwang S, Cai Y, Kim SJ, Xu M, Yang D, Guillot A, Feng D, Seo W, Hou X, Gao B, MicroRNA-223 Ameliorates Nonalcoholic Steatohepatitis and Cancer by Targeting Multiple Inflammatory and Oncogenic Genes in Hepatocytes, Hepatology, 70 (2019) 1150–1167. [PubMed: 30964207]

[27]. Li CX, Ling CC, Shao Y, Xu A, Li XC, Ng KT, Liu XB, Ma YY, Qi X, Liu H, Liu J, Yeung OW, Yang XX, Liu QS, Lam YF, Zhai Y, Lo CM, Man K, CXCL10/CXCR3 signaling mobilized-regulatory T cells promote liver tumor recurrence after transplantation, J Hepatol, 65 (2016) 944–952. [PubMed: 27245433]

[28]. Wei Y, Lao XM, Xiao X, Wang XY, Wu ZJ, Zeng QH, Wu CY, Wu RQ, Chen ZX, Zheng L, Li B, Kuang DM, Plasma Cell Polarization to the Immunoglobulin G Phenotype in Hepatocellular Carcinomas Involves Epigenetic Alterations and Promotes Hepatoma Progression in Mice, Gastroenterology, 156 (2019) 1890–1904 e1816. [PubMed: 30711627]

[29]. Chew V, Lai L, Pan L, Lim CJ, Li J, Ong R, Chua C, Leong JY, Lim KH, Toh HC, Lee SY, Chan CY, Goh BKP, Chung A, Chow PKH, Albani S, Delineation of an immunosuppressive gradient in

hepatocellular carcinoma using high-dimensional proteomic and transcriptomic analyses, Proc Natl Acad Sci U S A, 114 (2017) E5900–E5909. [PubMed: 28674001]

[30]. Liu RX, Wei Y, Zeng QH, Chan KW, Xiao X, Zhao XY, Chen MM, Ouyang FZ, Chen DP, Zheng L, Lao XM, Kuang DM, Chemokine (C-X-C motif) receptor 3-positive B cells link interleukin-17 inflammation to protumorigenic macrophage polarization in human hepatocellular carcinoma, Hepatology, 62 (2015) 1779–1790. [PubMed: 26235097]

[31]. Ueki S, Dhupar R, Cardinal J, Tsung A, Yoshida J, Ozaki KS, Klune JR, Murase N, Geller DA, Critical role of interferon regulatory factor-1 in murine liver transplant ischemia reperfusion injury, Hepatology, 51 (2010) 1692–1701. [PubMed: 20131404]

[32]. Du Q, Zhang X, Liu Q, Zhang X, Bartels CE, Geller DA, Nitric oxide production upregulates Wnt/beta-catenin signaling by inhibiting Dickkopf-1, Cancer Res, 73 (2013) 6526–6537. [PubMed: 24008318]

[33]. Spurrell JC, Wiehler S, Zaheer RS, Sanders SP, Proud D, Human airway epithelial cells produce IP-10 (CXCL10) in vitro and in vivo upon rhinovirus infection, Am J Physiol Lung Cell Mol Physiol, 289 (2005) L85–95. [PubMed: 15764644]

[34]. Zaheer RS, Proud D, Human rhinovirus-induced epithelial production of CXCL10 is dependent upon IFN regulatory factor-1, Am J Respir Cell Mol Biol, 43 (2010) 413–421. [PubMed: 19880820]

[35]. Majumder S, Zhou LZ, Chaturvedi P, Babcock G, Aras S, Ransohoff RM, p48/STAT-1alpha-containing complexes play a predominant role in induction of IFN-gamma-inducible protein, 10 kDa (IP-10) by IFN-gamma alone or in synergy with TNF-alpha, J Immunol, 161 (1998) 4736–4744. [PubMed: 9794404]

[36]. Cerami E, Gao J, Dogrusoz U, Gross BE, Sumer SO, Aksoy BA, Jacobsen A, Byrne CJ, Heuer ML, Larsson E, Antipin Y, Reva B, Goldberg AP, Sander C, Schultz N, The cBio cancer genomics portal: an open platform for exploring multidimensional cancer genomics data, Cancer Discov, 2 (2012) 401–404. [PubMed: 22588877]

[37]. Gao J, Aksoy BA, Dogrusoz U, Dresdner G, Gross B, Sumer SO, Sun Y, Jacobsen A, Sinha R, Larsson E, Cerami E, Sander C, Schultz N, Integrative analysis of complex cancer genomics and clinical profiles using the cBioPortal, Sci Signal, 6 (2013) pl1. [PubMed: 23550210]

[38]. Harada H, Fujita T, Miyamoto M, Kimura Y, Maruyama M, Furia A, Miyata T, Taniguchi T, Structurally similar but functionally distinct factors, IRF-1 and IRF-2, bind to the same regulatory elements of IFN and IFN-inducible genes, Cell, 58 (1989) 729–739. [PubMed: 2475256]

[39]. Yokota S, Yoshida O, Dou L, Spadaro AV, Isse K, Ross MA, Stolz DB, Kimura S, Du Q, Demetris AJ, Thomson AW, Geller DA, IRF-1 promotes liver transplant ischemia/reperfusion injury via hepatocyte IL-15/IL-15Ralpha production, J Immunol, 194 (2015) 6045–6056. [PubMed: 25964490]

[40]. Karin N, CXCR3 Ligands in Cancer and Autoimmunity, Chemoattraction of Effector T Cells, and Beyond, Front Immunol, 11 (2020) 976. [PubMed: 32547545]

[41]. Susek KH, Karvouni M, Alici E, Lundqvist A, The Role of CXC Chemokine Receptors 1–4 on Immune Cells in the Tumor Microenvironment, Front Immunol, 9 (2018) 2159. [PubMed: 30319622]

[42]. Finn RS, Qin S, Ikeda M, Galle PR, Ducreux M, Kim TY, Kudo M, Breder V, Merle P, Kaseb AO, Li D, Verret W, Xu DZ, Hernandez S, Liu J, Huang C, Mulla S, Wang Y, Lim HY, Zhu AX, Cheng AL, Investigators IM, Atezolizumab plus Bevacizumab in Unresectable Hepatocellular Carcinoma, N Engl J Med, 382 (2020) 1894–1905. [PubMed: 32402160]

[43]. Shergold AL, Millar R, Nibbs RJB, Understanding and overcoming the resistance of cancer to PD-1/PD-L1 blockade, Pharmacol Res, 145 (2019) 104258. [PubMed: 31063806]

[44]. Shao L, Hou W, Scharping NE, Vendetti FP, Srivastava R, Roy CN, Menk AV, Wang Y, Chauvin JM, Karukonda P, Thorne SH, Hornung V, Zarour HM, Bakkenist CJ, Delgoffe GM, Sarkar SN, IRF1 Inhibits Antitumor Immunity through the Upregulation of PD-L1 in the Tumor Cell, Cancer Immunol Res, 7 (2019) 1258–1266. [PubMed: 31239318]

[45]. Liang J, Wang L, Wang C, Shen J, Su B, Marisetty AL, Fang D, Kassab C, Jeong KJ, Zhao W, Lu Y, Jain AK, Zhou Z, Liang H, Sun SC, Lu C, Xu ZX, Yu Q, Shao S, Chen X, Gao M, Claret FX,

Ding Z, Chen J, Chen P, Barton MC, Peng G, Mills GB, Heimberger AB, Verteporfin Inhibits PD-L1 through Autophagy and the STAT1-IRF1-TRIM28 Signaling Axis, Exerting Antitumor Efficacy, Cancer Immunol Res, 8 (2020) 952–965. [PubMed: 32265228]

[46]. Taube JM, Klein A, Brahmer JR, Xu H, Pan X, Kim JH, Chen L, Pardoll DM, Topalian SL, Anders RA, Association of PD-1, PD-1 ligands, and other features of the tumor immune microenvironment with response to anti-PD-1 therapy, Clin Cancer Res, 20 (2014) 5064–5074. [PubMed: 24714771]

[47]. Tumeh PC, Harview CL, Yearley JH, Shintaku IP, Taylor EJ, Robert L, Chmielowski B, Spasic M, Henry G, Ciobanu V, West AN, Carmona M, Kivork C, Seja E, Cherry G, Gutierrez AJ, Grogan TR, Mateus C, Tomasic G, Glaspy JA, Emerson RO, Robins H, Pierce RH, Elashoff DA, Robert C, Ribas A, PD-1 blockade induces responses by inhibiting adaptive immune resistance, Nature, 515 (2014) 568–571. [PubMed: 25428505]

[48]. Ding L, Chen X, Xu X, Qian Y, Liang G, Yao F, Yao Z, Wu H, Zhang J, He Q, Yang B, PARP1 Suppresses the Transcription of PD-L1 by Poly(ADP-Ribosyl)ating STAT3, Cancer Immunol Res, 7 (2019) 136–149. [PubMed: 30401677]

[49]. Chow MT, Ozga AJ, Servis RL, Frederick DT, Lo JA, Fisher DE, Freeman GJ, Boland GM, Luster AD, Intratumoral Activity of the CXCR3 Chemokine System Is Required for the Efficacy of Anti-PD-1 Therapy, Immunity, 50 (2019) 1498–1512 e1495. [PubMed: 31097342]

[50]. Ren Y, Gu YK, Li Z, Xu GZ, Zhang YM, Dong MX, Wang Y, Zhou XB, CXCR3 confers sorafenib resistance of HCC cells through regulating metabolic alteration and AMPK pathway, Am J Transl Res, 12 (2020) 825–836. [PubMed: 32269715]

Highlights

- IRF-1 promotes CXCL10 expression at the transcriptional level by binding to specific IRF-1 response elements in the CXCL10 promoter.
- IRF-1 upregulates CXCR3 expression in HCC cells.
- IRF-1 exerts anti-proliferative and pro-apoptotic effects on HCC cells, which overcomes proliferation partly mediated by activating the CXCL10/CXCR3 autocrine axis.
- IRF-1 increases NK cells, NKT cells, and CD8+ T cells enrichment, and activates IFN-γ secretion in NK and NKT cells to induce tumor apoptosis through the CXCL10/CXCR3 paracrine axis.

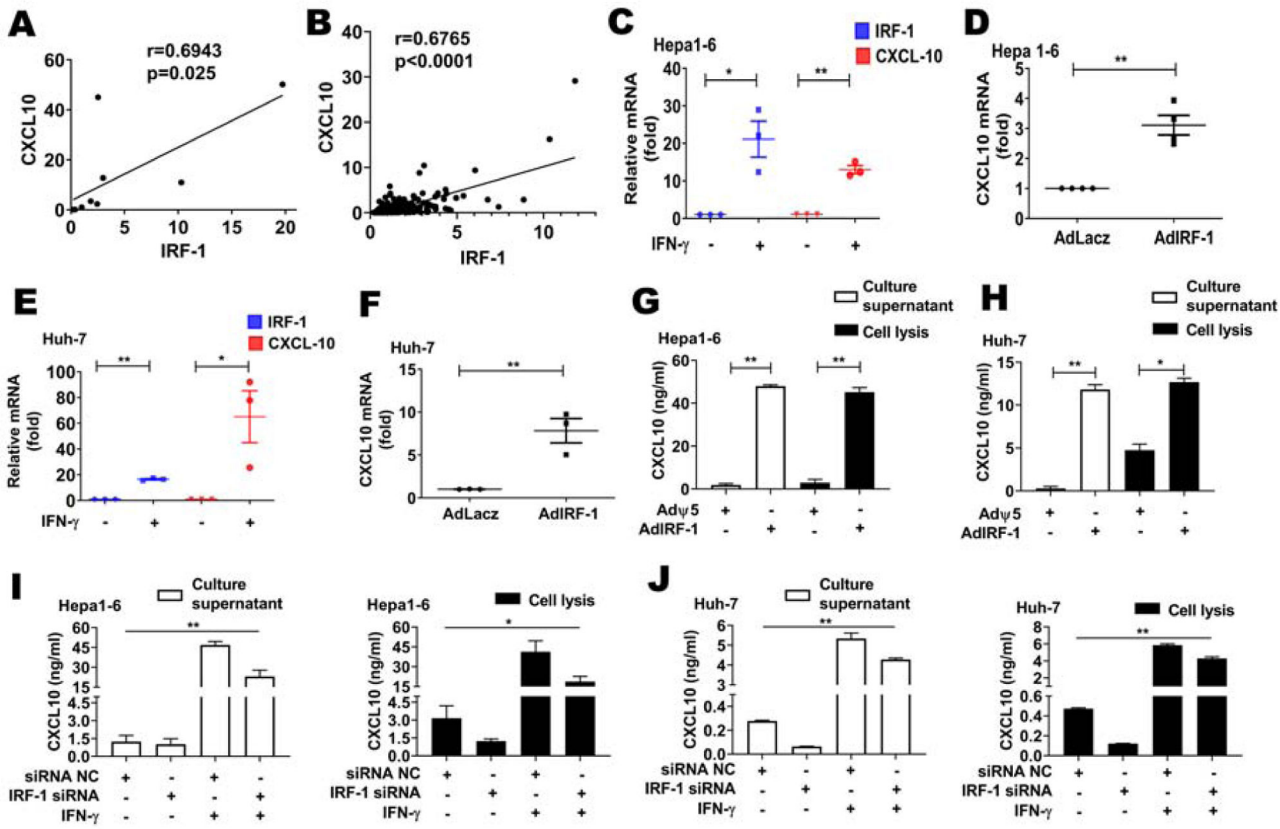

Figure 1. IRF-1 upregulates CXCL10 expression in HCC cells.

A) IRF-1 and CXCL10 mRNA expression are determined by qRT-PCR in tumor from HCC patients (n=10). B) Correlative analysis of IRF-1 and CXCL10 mRNA expression in HCC patients is based on TCGA database (n=360). Each data point (A & B) represents one patient. IRF-1 and CXCL10 mRNA expression are measured by qRT-PCR in Hepa1–6 cells (C, D) and Huh-7 (E, F) induced by mouse IFN-γ (50 u/ml) / human IFN-γ (100 u/ml) for 24 h, or infected by mouse / human AdIRF-1 (50 MOI) for 48 h, respectively. Each data point (C, D, E & F) represents an independent experiment (n=3–4). CXCL10 protein expression in cell lysis and culture supernatant are detected by ELISA in Hepa1–6 cells (G, I) and Huh-7 cells (H, J). The cells are infected by mouse / human AdIRF-1 (50 MOI) for 48 h (G, H). Cells are transfected with IRF-1 siRNA or negative control (NC) for 48 h with or without mouse IFN-γ (50 u/ml) / human IFN-γ (100 u/ml) for 12 h, respectively (I, J). ELISA assay data represent the means ± SEM of two samples and are representative of two independent experiments with similar results. The statistical analyses on four different groups (I, J) are performed by One-way ANOVA. The t test is used to compare between two different groups, *p<0.05, **p<0.01.

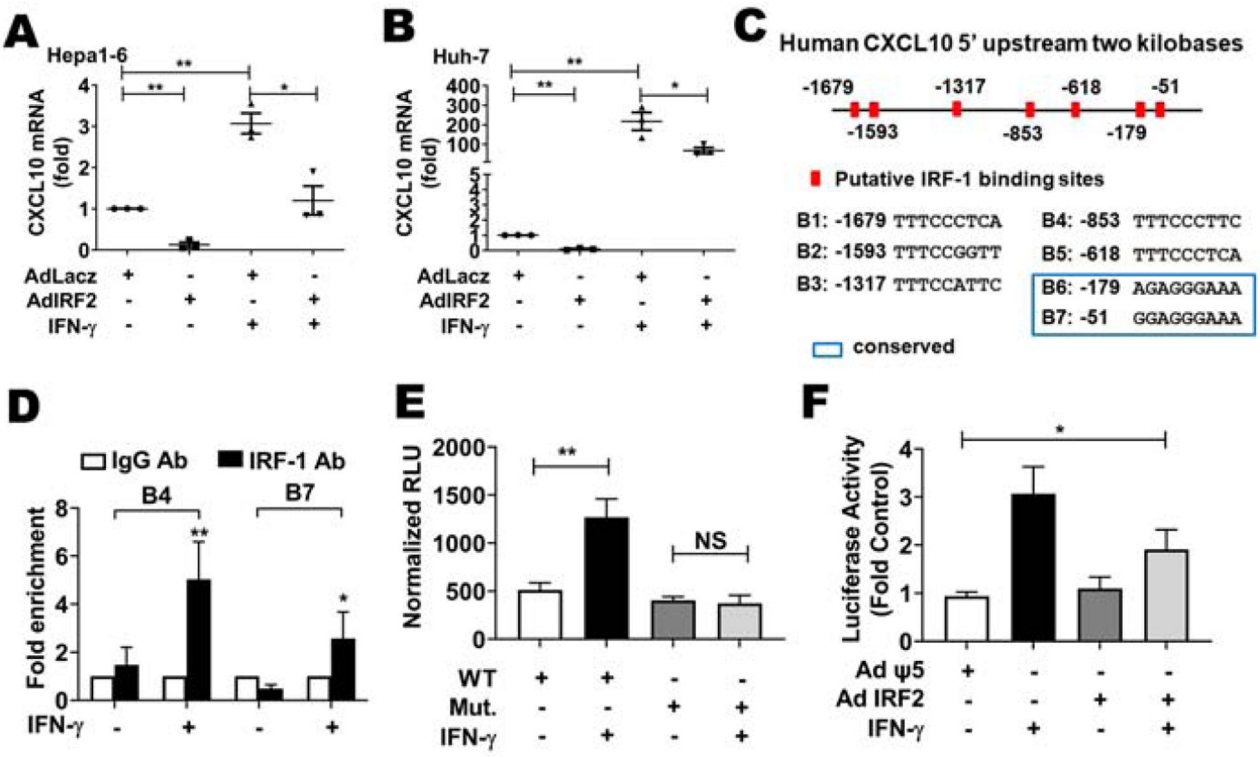

Figure 2. IRF-1 promotes CXCL10 transcription.

CXCL10 mRNA expression is defined by qRT-PCR in Hepa1–6 cells (A) and Huh-7 cells (B) infected by mouse / human AdIRF-2 (50 MOI) for 48 h with or without mouse IFN-γ (50 u/ml) / human IFN-γ (100 u/ml) for 12 h, respectively. C) Schematic representation of IRF-1 binding sites in the human CXCL10 promoter region as predicted by PROMO bioinformatics software. D) ChIP assay is performed with IgG or anti IRF-1 antibody in cell lysis from Huh-7 cells which are induced by human IFN-γ (250 u/ml) for 6 h. The qPCR analyses of immunoprecipitated DNA are conducted using the primers which are designed to amplify the indicated region of the CXCL10 promoter. Each data point (A & B) represents an independent experiment (n=3). Data (A, B & D) represent the mean ± SD, *p<0.05, **p<0.01. ChIP-qPCR assay results shown are statistical difference from four independent experiments. E) Luciferase activity from IFN-γ (250 u/ml) induced HepG2 cells transfected with wild type (WT) CXCL10 promoter construct (but not mutated ISRE CXCL10 promoter construct) is significantly increased (**p<0.01, NS not significant). F) IRF-2 significantly reduces luciferase activity from IFN-γ stimulated wild type CXCL10 promoter construct (*p<0.05 by ANOVA). Luciferase assays shown are representative of four experiments with similar results.

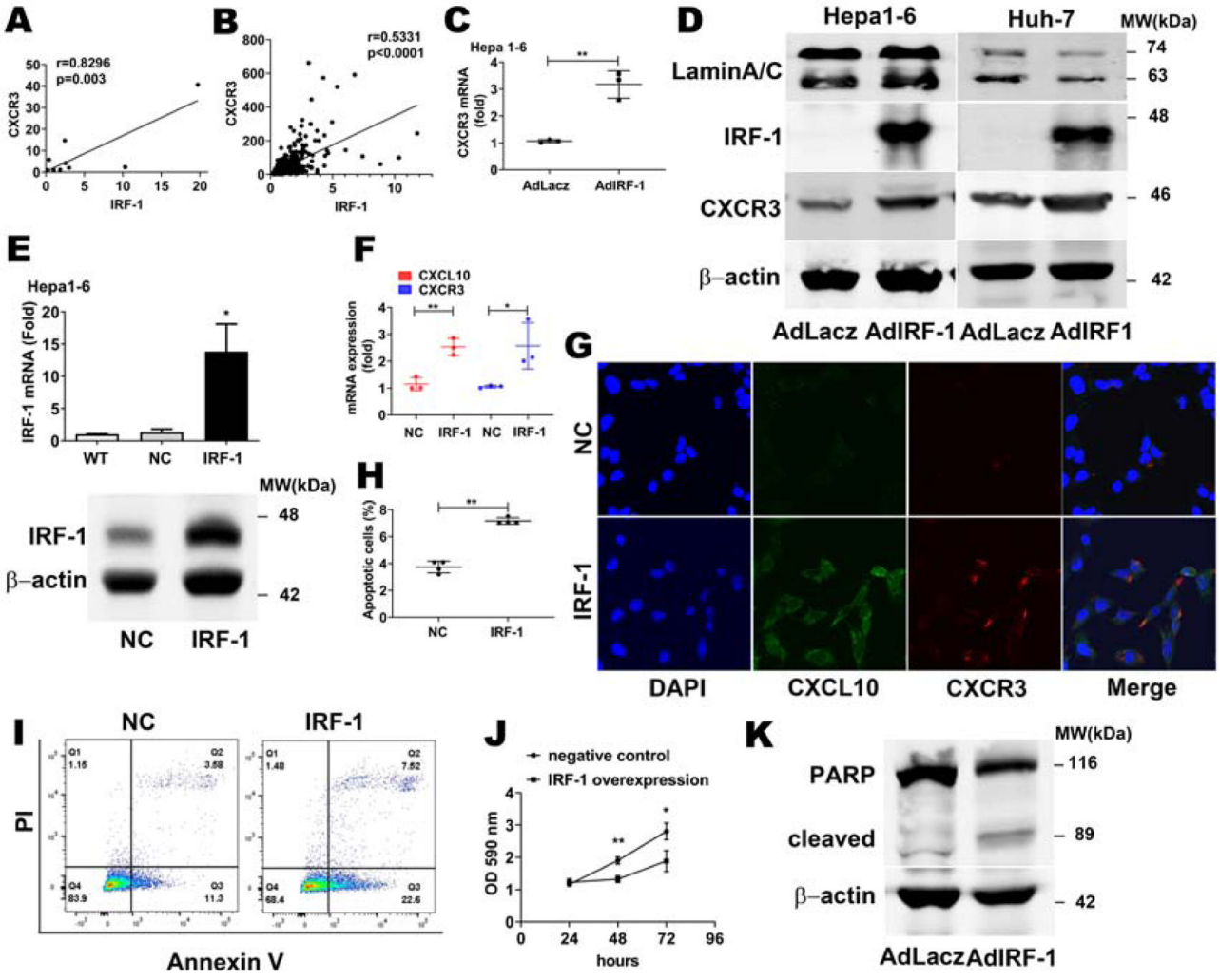

Figure 3. IRF-1 has anti-proliferative and pro-apoptotic effect on HCC cells.

A) IRF-1 and CXCR3 mRNA expression are determined by qRT-PCR in tumor from HCC patients (n=10). B) Correlative analysis of IRF-1 and CXCR3 mRNA expression in HCC patients is based on TCGA database (n=360). Each data point (A & B) represents one patient. CXCR3 mRNA (C) and protein (D) expression are respectively measured by qRT-PCR and western blot in Hepa1–6 cells and Huh-7 cells infected by mouse / human AdIRF-1 (50 MOI) for 48 h. E) IRF-1 mRNA (upper) and total protein (lower) expression are respectively analyzed by qRT-PCR and western blot in HCC cells stably overexpressing IRF-1 (IRF-1) vs. negative control (NC) and wild type (WT). The qRT-PCR data are presented as mean ± SEM and shown statistical difference from three independent experiments. F, G) CXCL10 and CXCR3 mRNA (F) and protein (G) expression are respectively determined by qRT-PCR and immunofluorescent staining in IRF-1 vs. NC (×400 magnification). H, I) The statistical summary of apoptotic Hepa1–6 cells rate (H) and representative images (I) of FACS assay for apoptotic (Annexin V+PI+) cells rate in Hepa1–6 cells expressing IRF-1 vs. NC. Each data point (C, F, & H) represents an independent experiment. Data represent mean ± SD. J) MTT assay for cells expressing IRF-1 vs. NC at different time points. The data are presented as the means ± SEM of six samples and are

representative of two independent experiments with similar results. K) Western blot analysis for cleaved PARP in Huh-7 cells infected by human AdIRF-1 (50 MOI) for 48 h. Western blot and immunofluorescent results shown are representative image from two independent experiments. *p<0.05, **p<0.01.

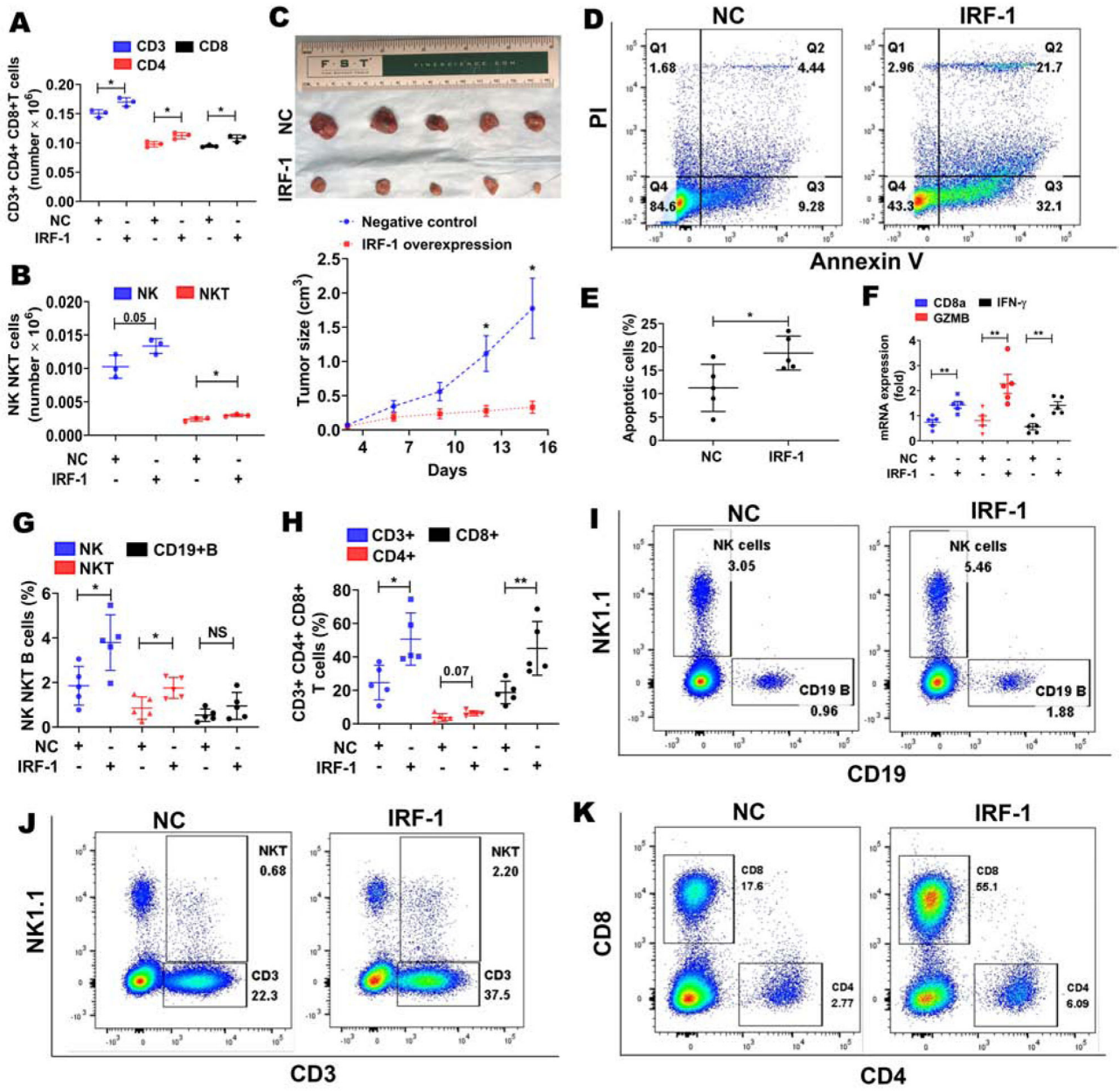

Figure 4. IRF-1 recruits immune cells to enhance apoptosis in murine HCC tumor.

A, B) The statistical summary of cells count in CD3+, CD4+, CD8+ T cells, and NK and NKT cells in the medium of Hepa1–6 cells overexpressing IRF-1 (IRF-1) vs. negative control (NC) in the lower chamber of transwell plate. C) Tumor images (upper) and growth curves (lower, mean ± SEM) of murine HCC tumor overexpressing IRF-1 (lower) vs. negative control (upper). D) Representative images of FACS assay for apoptotic (Annexin V +PI+) cell rate in single cell suspensions prepared from same volume of tumors expressing IRF-1 vs. NC. E) The statistical summary of apoptotic tumor cells rate in tumors expressing IRF-1 vs. NC. F) qRT-PCR analysis for CD8a, GZMB and IFN-γ mRNA expression in tumors expressing IRF-1 vs. NC. G, H) The statistical summary of NK cells, NKT cells and CD19+ B cells rate, as well as CD3+, CD4+ and CD8+ T cells rate in tumors expressing

IRF-1 vs. NC. Representative images of FACS assay for NK cells or CD19+ B cells rate (I), NKT cells rate (J), CD4+ or CD8+ T cells rate (K) in single cell suspensions prepared from same volume of tumors expressing IRF-1 vs. NC. Each data point (A, B) represents an independent experiment (n=3). Each data point (E, F, G & H) represents one mouse (n=5). Data represent mean ± SD, *p<0.05, **p<0.01. (NS, no significant).

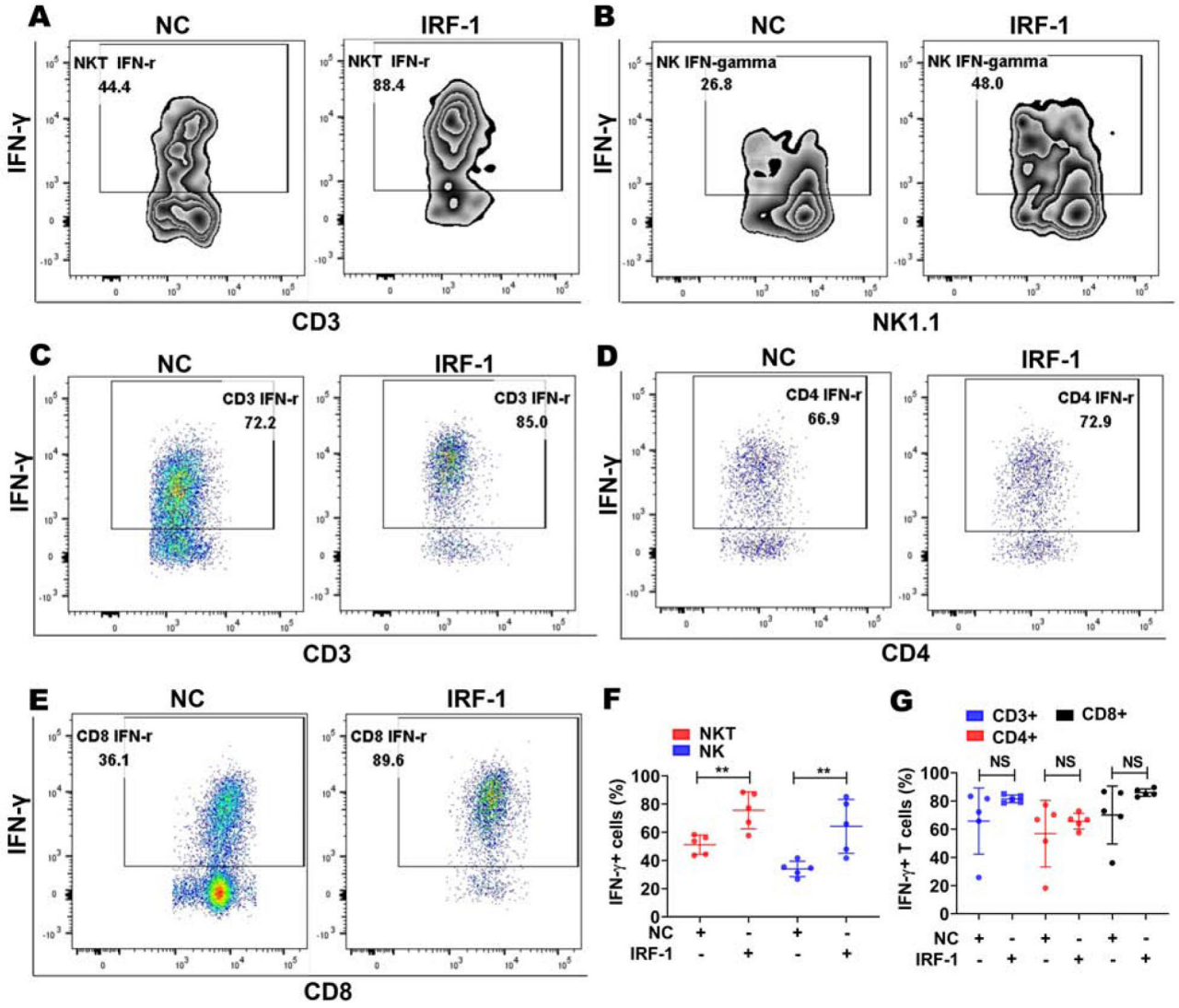

Figure 5. IRF-1 promotes IFN-γ expression in infiltrating NK cells and NKT cells.

Representative images of FACS assay for IFN-γ expression in NKT cells (A), NK cells (B), CD3+T cells (C), CD4+T cells (D) and CD8+ T cells (E) of single cell suspensions prepared from same volume of tumors overexpressing IRF-1 (IRF-1) vs. negative control (NC). (F, G)The statistical summary of IFN-γ expression cells rate in tumors with IRF-1 vs. NC. Each data point (F & G) represents one mouse (n=5). Data represent mean ± SD, **p<0.01. (NS, no significant).

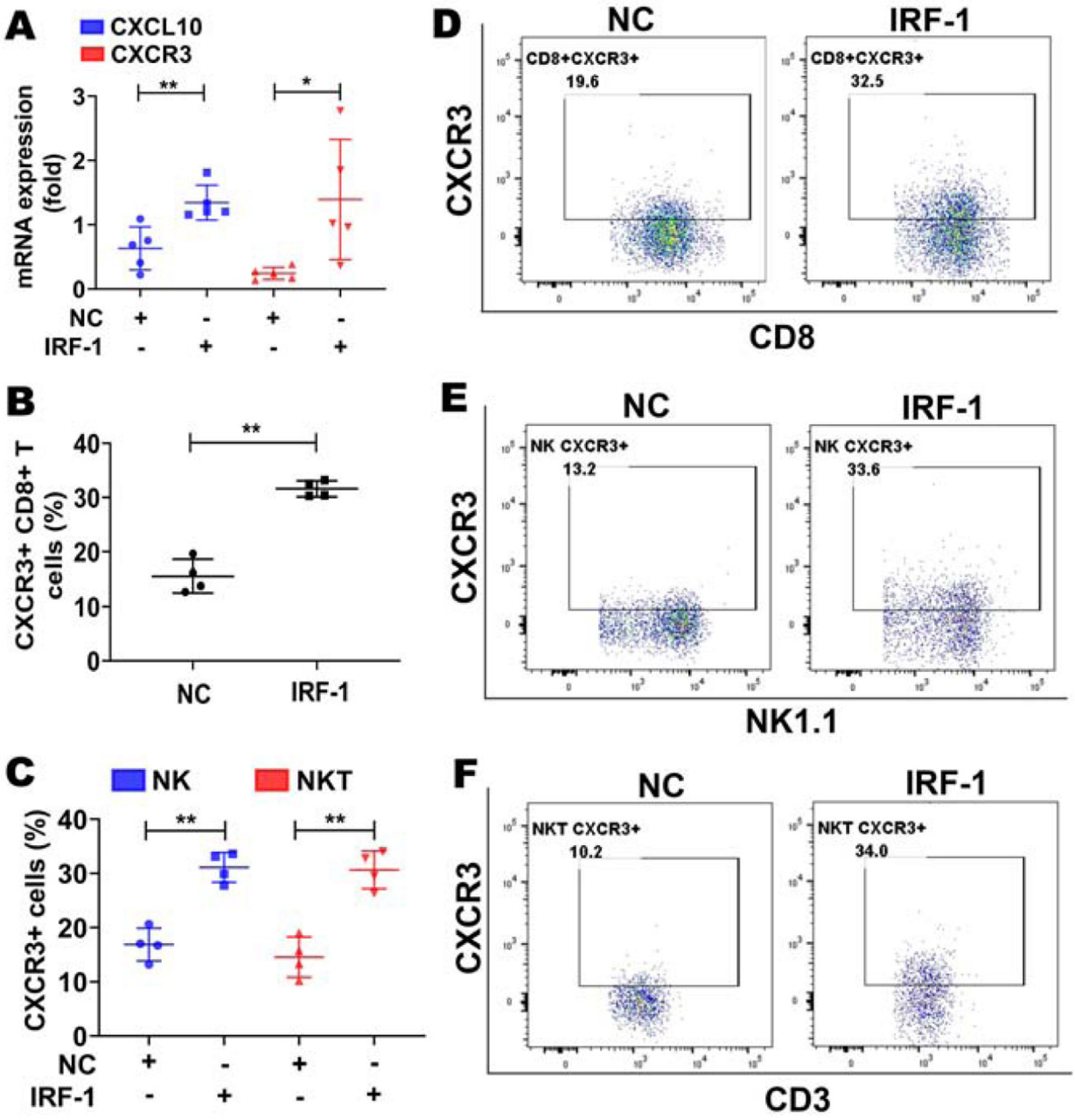

Figure 6. IRF-1 recruits immune cells via CXCL10/CXCR3 axis in murine HCC tumor.

A) qRT-PCR analysis for CXCL10 and CXCR3 mRNA expression in murine HCC tumors overexpressing IRF-1 (IRF-1) vs. negative control (NC). (B, C) The statistical summary of CXCR3 positive cell rate in CD8+T cells, NK cells and NKT cells in single cell suspension from same volume of tumors expressing IRF-1 vs. NC. Representative images of FACS assay for CXCR3 positive cell rate in CD8+T cells (D), NK cells (E) and NKT cells (F) in tumors expressing IRF-1 vs. NC. Each data point (A, B & C) represents one mouse (n=4–5). Data represent mean ± SD, *p<0.05, **p<0.01.

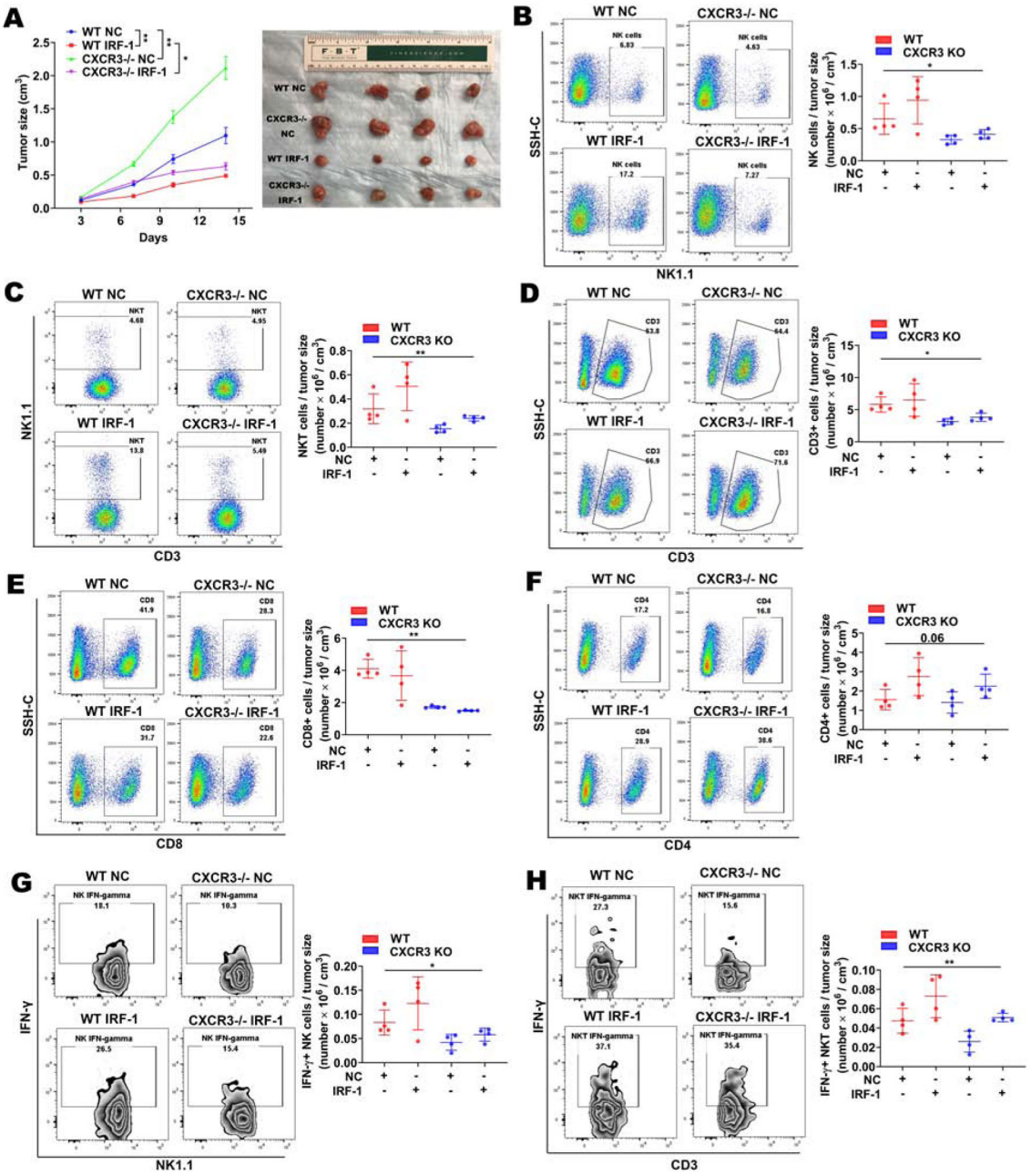

Figure 7. CXCR3 knock out attenuates immune cells recruitment and IFN-γ expression induced by IRF-1 overexpressing in murine HCC tumor.

A) Tumor image (right) and growth curves (left, mean ± SEM) of murine HCC tumor with negative control (NC) grown in wild type (WT) mice (row 1, blue, n=4) and CXCR3 KO (CXCR3−/−) mice (row 2, green, n=4), as well as tumor overexpressing IRF-1 (IRF-1) grown in WT mice (row 3, red, n=4) and CXCR3−/− mice (row 4, purple, n=4). B-F) Representative images and statistical summary of FACS assay for NK cells (B), NKT cells (C), CD3+ T cells (D), CD8+ T cells (E), and CD4+ T cells (F) number per cubic centimeter of tumor expressing IRF-1 vs. NC subcutaneously grown in WT or CXCR3−/− mice, respectively. G, H) Representative images and statistical summary of FACS assay for IFN-γ

+ NK cells (G) and NKT cells (H) number per cubic centimeter of tumor expressing IRF-1 vs. NC subcutaneously grown in WT or CXCR3−/− mice, respectively. Each data point represents one mouse (n=4, each group). The statistical analyses on four different groups are performed by One-way ANOVA. The t test is used to compare between two different groups. Data represent mean ± SD, *p<0.05, **p<0.01.

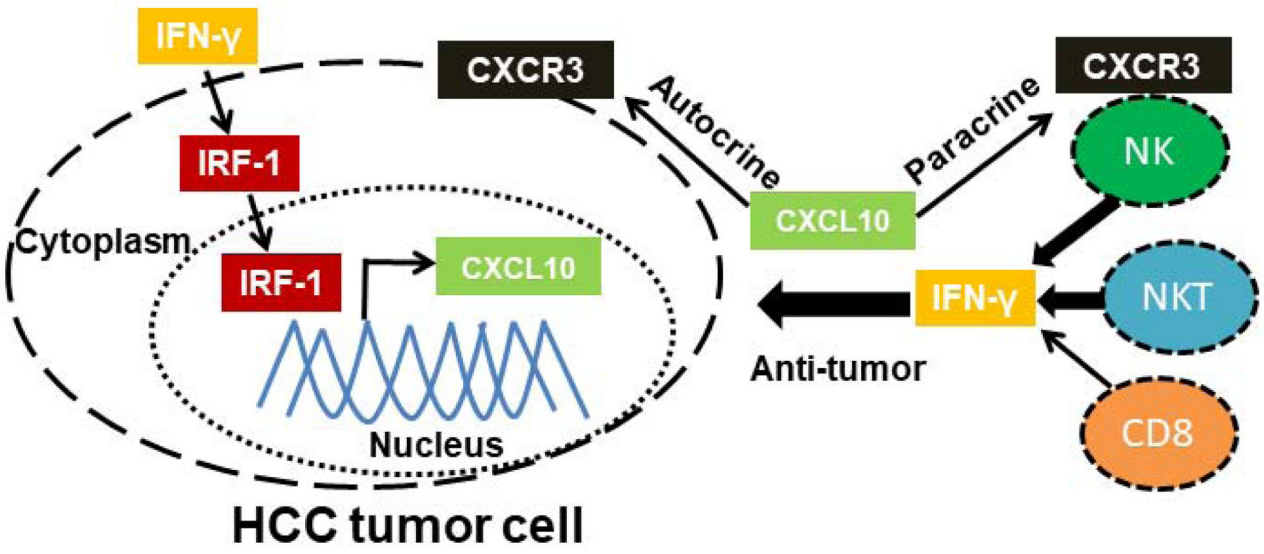

Figure 8. Tumor derived IRF-1 recruits and activates immune cells to play anti-tumor effect on HCC through CXCL10/CXCR3 axis.

IFN-γ (yellow) induces IRF-1 (red) expression in HCC cells. IRF-1 upregulates CXCL10 (green) expression through binding to the promoter of CXCL10. The induced CXCL10 binds to CXCR3 (black) in the tumor cells via autocrine axis. Meanwhile, CXCL10 binds to CXCR3 in the NK cells (NK), NKT cells (NKT), and CD8+T cells (CD8), as well as increases IFN-γ expression in NK and NKT cells to play anti-tumor function on HCC cells.